

Guk Bae Kim · Sang Joon Lee

X-ray PIV measurements of blood flows without tracer particles

Received: 15 November 2005 / Revised: 19 January 2006 / Accepted: 31 March 2006 / Published online: 27 April 2006
© Springer-Verlag 2006

Abstract We analyzed the non-Newtonian flow characteristics of blood moving in a circular tube flow using an X-ray PIV method and compared the experimental results with hemodynamic models. The X-ray PIV method was improved for measuring quantitative velocity fields of blood flows using a coherent synchrotron X-ray. Without using any contrast media, this method can visualize flow pattern of blood by enhancing the phase-contrast and interference characteristics of blood cells. The enhanced X-ray images were achieved by optimizing the sample-to-scintillator distance, the sample thickness, and hematocrit in detail. The quantitative velocity fields of blood flows inside opaque conduits were obtained by applying a two-frame PIV algorithm to the X-ray images of the blood flows. The measured velocity data show typical features of blood flow such as the yield stress and shear-thinning effects.

1 Introduction

Most flow visualization techniques using visible light can be employed only for transparent fluids. They are unsuitable to visualize human blood flow due to RBCs (red blood cells) occupying about 37–45% of the whole blood. When the thickness of blood sample exceeds several hundred micrometers, the blood becomes opaque for visible light, making difficult to visualize the blood flow with optical methods. For the case of *transparent* micrometers, we can visualize a blood flow with very small depth (several tens of micrometers) by tracing RBCs or tracer particles seeded in the blood using a visible light (Park et al. 2004). However, most important

hemodynamic phenomena related with circulatory vascular diseases occur in the blood vessels of several millimeters or even larger in diameters. Therefore, most conventional flow visualization methods cannot be used for direct visualization of blood flows and for investigating hemodynamic phenomena, even when transparent substitutes for blood vessels are used.

On the other hand, most nondestructive medical instruments capable of observing the internal structures of opaque objects have not been developed yet to the level of observing internal flows of opaque objects. Therefore, direct visualization of a blood flow in an opaque conduit is not easy for conventional clinical devices.

Therefore, there is a long-term demand for developing a new advanced measurement technique that can extract quantitative flow information of blood flows in arteries, veins, capillaries, and lymphatic vessels. To resolve the limitations encountered in conventional clinical instruments and particle image velocimetry (PIV) velocity field measurement techniques, we developed an X-ray PIV technique (Lee and Kim 2003) and found its feasibility of visualizing a blood flow (Lee and Kim 2005). In this study, we investigated the optical characteristics of blood for a coherent synchrotron X-ray more systematically with varying several parameters such as distance between the sample and scintillator, sample thickness and hematocrit, compared with our previous works (Lee and Kim 2005). In addition, we analyzed the non-Newtonian flow characteristics of blood moving in a circular tube and compared the experimental results with hemodynamic models.

2 Experiments

2.1 Characteristics of blood on the X-ray imaging method

To visualize blood flow inside an opaque conduit and analyze the flow characteristics quantitatively, we com-

G. B. Kim · S. J. Lee (✉)
Department of Mechanical Engineering,
Pohang University of Science and Technology,
San 31, Hyo-Ja Dong, Pohang 790-784, Korea
E-mail: sjlee@postech.ac.kr
Tel.: +82-54-2792169
Fax: +82-54-2793199

bined an X-ray micro-imaging technique and a PIV technique. The third generation synchrotron radiation source of the PLS (Pohang Light Source, Pohang, Korea) was used in this study. The high coherence of this light source offers various approaches to radiology (Snigirev et al. 1995; Chapman et al. 1997; Pogany et al. 1997; Nugent et al. 1996). Several imaging techniques utilizing coherent light sources, such as holography and interferometry, have been studied. In addition, some phase contrast imaging methods have been developed (Hu et al. 1998; Spanne et al. 1999; Gureyev et al. 1999).

Two problems, however, have to be solved for applying the X-ray PIV technique to X-ray images of blood flows. At first, velocity field information is commonly extracted from flow images by tracking tracer particles seeded into the flow. However, the adulteration of blood with artificial tracer particles may alter the biochemical and fluidic characteristics of the blood, and may cause biological damage on the blood. Therefore, for investigating real blood flows, we should extract velocity information from the blood flow itself without adding any tracer particles. Second, because the biological specimens composed of low-density elements are transparent to hard X-rays, the conventional absorption-contrast X-ray imaging method is ineffective (Kagoshima et al. 2001). In addition, because the optical properties of RBCs and plasma are so similar, it is not easy to discriminate blood cells clearly even using the phase-contrast X-ray imaging method.

To resolve these problems, we captured fringe patterns of blood flow illuminated with a coherent synchrotron X-ray beam. The coherent X-rays induce classic Fresnel edge diffraction in radiological images. This Fresnel edge diffraction pattern, which consists of alternating bright and dark fringes, is formed as a result of interference between two differently phase-shifted waves passing through an object. The fringes in the captured X-ray images make it easy to discern the edges of specimens (such as RBCs). In general, the fringe patterns become clearer as the sample-to-scintillator distance d is increased. In the present experiments, we obtained X-ray images of blood flow using the propagation-based phase-contrast method after optimizing the sample(blood)-to-scintillator distance d .

Figure 1 shows the X-ray images of RBCs monolayer at four different distances d . For the X-ray images of RBCs, we used an unmonochromatic beam at 7B2 beam line of PLS. The lateral resolution is less than $0.7 \mu\text{m}$ and the size of source in the vertical and horizontal directions are 45 and $120 \mu\text{m}$, respectively. The beam characteristics and performance of this experimental beamline are described in Je et al. (2004).

An optical image of the same RBC monolayer is included for comparison. The scale bar corresponds to $10 \mu\text{m}$ and all images were captured under the same magnification. In the optical image (Fig. 2a), individual RBCs are clearly visualized. However, as shown in Fig. 2b, c, the RBCs cannot be discerned in the X-ray images obtained at small sample-to-scintillator distances

($d = 1$ and 3 cm). When d is increased beyond 3 cm , RBC fringe patterns become clearer (Fig. 2d, e). Comparison of the size of RBCs appeared in the optical image and the fringe patterns in the X-ray images confirm that the fringe patterns originate directly from the RBCs. It is worth noting that the phase-contrast enhancement method can visualize blood cells without magnification optics such as a zone-plate, a Kirkpatrick–Baez mirror, or a compound refractive lens.

In this study, we systematically investigated the effects of two parameters, the sample-to-scintillator distance and the sample thickness, on the fringe patterns appeared on X-ray images of tested blood samples. Figure 2 shows X-ray images of blood flow captured using the phase-contrast/interference-based edge enhancement method. Due to the phase-contrast enhancement, the blood image becomes to show flow pattern with increasing the distance d . When d is larger than 8 cm , the fringe pattern is recognizable for all thickness tested in this study. When the distance d is over 40 cm , however, the blood patterns begin to be blurry slightly due to excessive phase-contrast enhancement. Nevertheless, the blood pattern images are still reasonably recognizable inside the solid-line box, suitable for applying PIV algorithm to extract velocity field information. In the viewpoint of interference enhancement, all patterns of blood sample with thickness $t = 0.3\text{--}10 \text{ mm}$ are recognizable, if the sample-to-scintillator distance d is selected properly. In particular, the X-ray images of a blood sample with thickness 10 mm show good permeability of X-ray beam, even though visualization of such a sample of large thickness using a synchrotron X-ray source would generally be difficult. From these results, we can see that this X-ray imaging technique can be applied to blood flows in large blood vessels.

To investigate the effect of blood composition (RBCs and plasma) on X-ray imaging, we captured X-ray images of blood samples with varying different RBC concentration under the same experimental conditions of $d = 20 \text{ cm}$ and $t = 2 \text{ mm}$. The volume fractions of RBCs (hematocrit H) tested in this study are $H = 0.0, 2.5, 5.0, 7.5, 10.0, 20.0, 30.0, 40.0, 50.0, 60.0, 70.0, 80.0, 90.0,$ and 100.0% . Here, $H = 0\%$ corresponds to pure plasma and $H = 100\%$ to pure RBCs. In general, $H = 37\text{--}45\%$ for whole blood of a human being. As can be seen in Fig. 3, the X-ray images of blood samples with $H = 0\text{--}10.0\%$ do not show discernable fringe patterns. Distinct fringe patterns are obtained in the range of $H = 20.0\text{--}80.0\%$. Interestingly, the fringe pattern disappears for $H \geq 90.0\%$, suggesting that a certain amount of plasma, which differs from RBCs in terms of refractive index and density, is required to enhance the RBC fringe pattern. Blood with high hematocrit may be considered to have nearly a single refractive index. Therefore, no phase-contrast, interference or refraction is induced at the edges of RBCs for such samples. Fortunately, however, the hematocrit of greatest interest for researchers working in the fields of

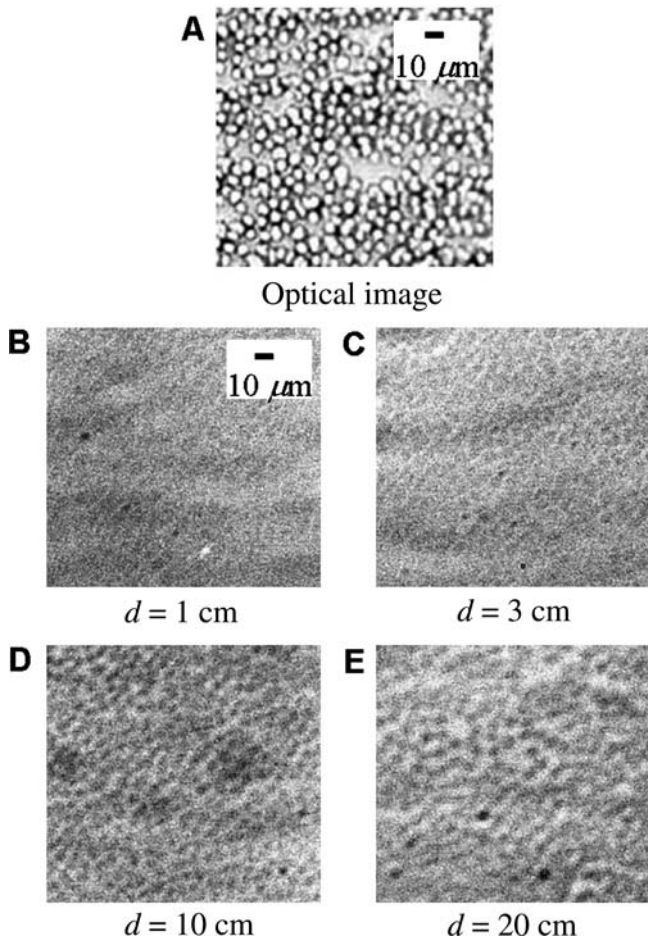


Fig. 1 X-ray images of RBC monolayer using the phase-contrast enhancement

hemodynamics and circulating diseases is ranged from $H = 20.0$ to 80.0% .

2.2 X-ray PIV measurements of blood flow

Using the phase-contrast and interference-based edge enhancement methods of synchrotron X-ray microimaging, it is possible to directly visualize blood flow in an opaque conduit without seeding any tracer particles or contrast materials. The experiments were carried out at 7B2 beam line of PLS. A schematic diagram of the experimental setup for the X-ray PIV measurements is shown in Fig. 4. The X-ray images were captured with a cooled CCD camera (PCO Sensicam) with $1,280 \times 1,024$ pixels resolution, after converting the X-rays to visible light using a thin CdWO_4 scintillator crystal. The spatial resolution (Δy and Δz) of the CCD camera was about $0.67 \mu\text{m}$ and the field of view was about $514 \times 686 \mu\text{m}^2$ in physical size, when the camera was coupled with a $10\times$ objective lens.

Because the X-ray beam was supplied continuously, we installed a mechanical shutter to generate a pulse-

type X-ray beam for PIV measurements. A delay generator was used to synchronize the mechanical shutter and the CCD camera. A syringe pump was employed to supply blood into the microchannel installed vertically. We captured X-ray images of blood flow in a rectangular-shaped opaque microchannel of width $490 \mu\text{m}$ and depth $1,390 \mu\text{m}$ under the optimized conditions of the sample-to-scintillator distance (40 cm) and sample thickness ($1,390 \mu\text{m}$). By applying a two-frame cross-correlation PIV algorithm to the phase-contrast/interference-enhanced X-ray images of the blood flow, we could obtain instantaneous velocity fields without any artificial tracer particles. Each X-ray image was divided into many small interrogation windows of $13 \times 13 \mu\text{m}^2$ in physical size. The speckle pattern appeared in X-ray images shows different displacement with respect to the distance from the wall. The length of displacement increases with going from the wall to the center region of the channel. This indicates that the displacement of speckle pattern contains information on transportation of blood cells.

The mean velocity field was obtained by ensemble averaging 200 consecutive instantaneous velocity fields statistically. The measured streamwise mean velocity field is shown in Fig. 5 (Lee and Kim 2005). The flow speed increases with going toward the channel center from the channel wall. This velocity field is similar to the velocity distribution typically observed in a macro-sized channel of a rectangular cross-section. This quantitative velocity field result shows the reliability of X-ray PIV method for measuring blood flows.

We also investigated blood flow inside an opaque tube with a circular cross-section. This is a realistic application of the X-ray PIV method for analyzing the non-Newtonian characteristics of real blood flows. Inner diameter of the opaque tube was 2.77 mm and blood was injected by a syringe pump at a flow rate of $50 \mu\text{l}/\text{min}$. Exposure time for acquiring each X-ray image was 20 ms . Figure 6 shows a typical streamwise mean velocity profile extracted from the mean velocity field data along a horizontal line. From the results of mean velocity profiles of real blood flow, we compared the experimental velocity profile with hemorheologic models of blood flow. As far as we surveyed, there is no quantitative flow information of real blood flow measured non-invasively with a high spatial resolution. It is the first trial to evaluate the hemorheologic models with the experimental results. Figure 6 shows that the measured velocity profile is well agreed with the velocity profile suggested by Casson model (Syoten 1981; Macosko 1994). The typical parabolic velocity profile of Newtonian flow has some discrepancy with the experimental result. The diameter of center potential region in which no velocity gradient exists due to the yield stress of blood is $r_c/R = 0.044$. Conclusively, we found that the X-ray PIV method can be used for revealing various hemodynamic phenomena experimentally.

Fig. 2 X-ray images of blood captured using the phase-contrast/interference-based enhancement method

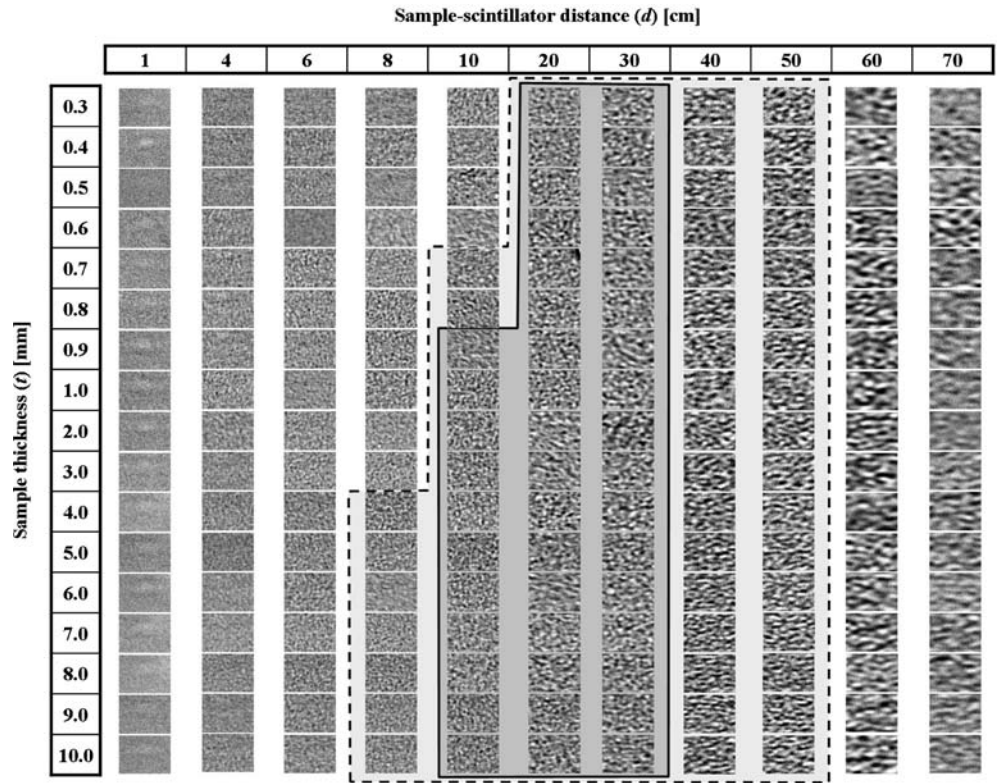
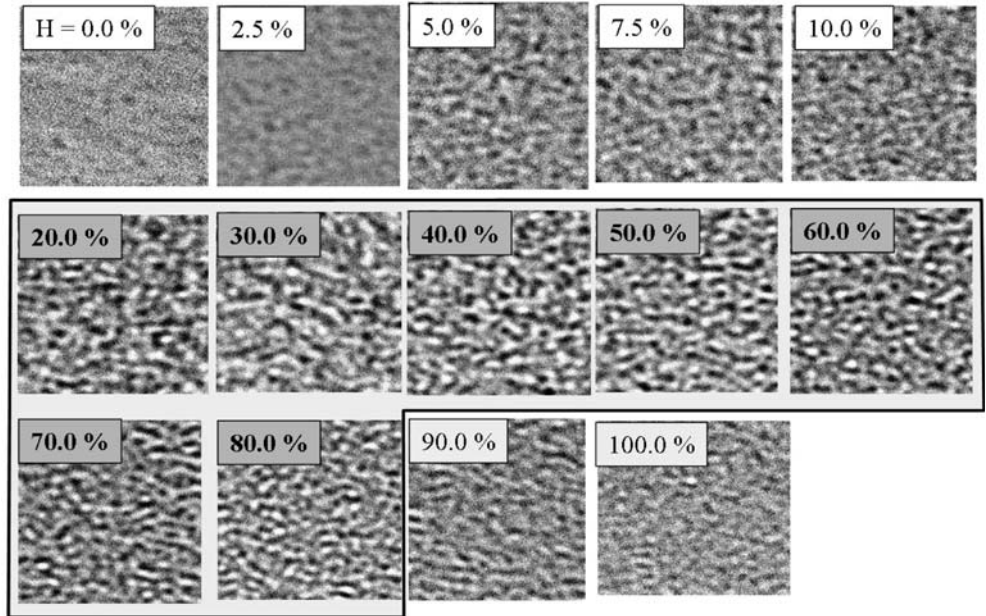


Fig. 3 Blood pattern images with respect to hematocrit ($d = 20$ cm, $t = 2$ mm)



3 Conclusion

In this study, we optimized the experimental condition such as sample(blood)-to-scintillator distance, sample(blood) thickness, and hematocrit to acquire suitable X-ray images of blood flow for PIV measurements. As

the sample-to-scintillator distance increases, the flow pattern becomes detectable with the induced phase-contrast enhancement. The optimum distance for blood sample was about 10–40 cm. The developed X-ray imaging technique was found to give suitable flow images for blood samples thicker than 1 mm. For hematocrit in the range of 20.0–80.0%, the X-ray

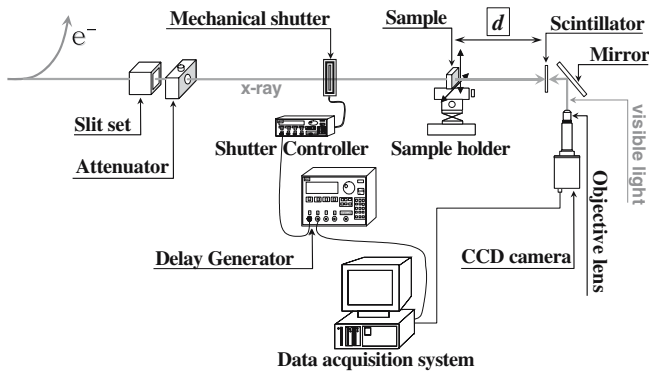


Fig. 4 Schematic diagram of X-ray PIV system

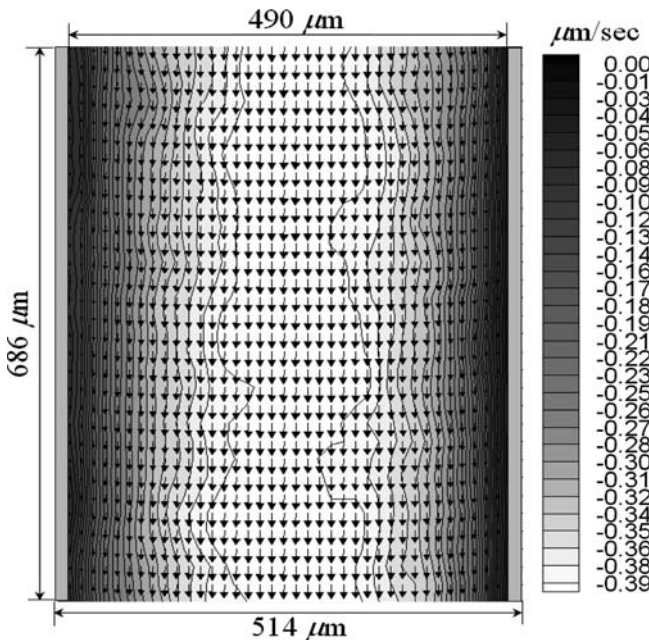


Fig. 5 Streamwise mean velocity field of blood flow measured in an opaque microchannel

blood pattern is also clearly visible. The X-ray PIV technique was applied to blood flows in an opaque rectangular microchannel. The measured velocity field data are reasonably agreed with the theoretical results. We also applied the X-ray PIV method to measure blood flow in a circular tube for analyzing its non-Newtonian flow characteristics. The X-ray PIV results are well matched with the Casson's hemorheological model. The X-ray PIV method has a strong potential for visualizing blood samples non-invasively to obtain detailed flow information such as flow rate, spatial distributions of velocity, and shear stress. We hope the developed X-ray PIV method can be used for investigating various hemodynamic phenomena for which the hemodynamics and the pathology of circulatory diseases play a key role.

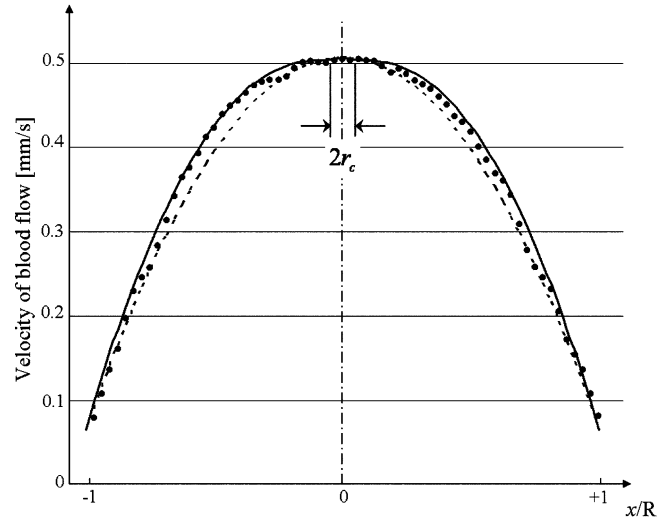


Fig. 6 Comparison of streamwise mean velocity profile of a blood flow inside a circular tube. *Dotted line* represents X-ray PIV result, *dashed line* represents parabolic curve fitting on the X-ray PIV result, and *continuous line* represents the Casson model fitting on the X-ray PIV result

Acknowledgement Experiments at the 7B2 beamline of PLS were supported in part by MOST and POSTECH. This work was also supported by MOST (KOSEF) through grant no. (R01-2004-000-10500-0) from the Basic Research Program and Systems Biodynamics Research Center.

References

- Chapman D, Thomlinson W, Johnston RE, Washburn D, Pisano E, Gmur N, Zhong Z, Menk R, Arfelli F, Sayers D (1997) Diffraction enhanced X-ray imaging. *Phys Med Biol* 42:2015–2025
- Gureyev TE, Raven C, Snigirev A, Snigireva I, Wilkins SW (1999) Hard X-ray quantitative non-interferometric phase-contrast microscopy. *J Phys D* 32:563–567
- Hu ZH, Thomas PA, Snigirev A, Snigireva I, Souvorov A, Smith PGR, Ross GW, Teat S (1998) Phase-mapping of periodically domain-inverted LiNbO₃ with coherent X-rays. *Nature (London)* 392:690–693
- Je JH, Baik S, Kim HS, Jeong MH, Lee CS, Hwu Y, Margaritondo G (2004) International consortium on phase contrast imaging and radiology beamline at the Pohang light source. *Rev Sci Instrum* 75:4355–4358
- Kagoshima Y, Ibuki T, Yokoyama Y, Tsusaka Y, Matsui J, Takai K, Aino M (2001) 10 keV X-ray phase-contrast microscopy of observing transparent specimens. *Jpn J Appl Phys* 40:L1190–L1192
- Lee SJ, Kim GB (2003) X-ray particle image velocimetry for measuring quantitative flow information inside opaque objects. *J Appl Phys* 94:3620–3623
- Lee SJ, Kim GB (2005). Synchrotron micro-imaging technique for measuring the velocity field of real blood flows. *J Appl Phys* 97:064701
- Macosko CW (1994) Rheology principles, measurements and applications. Wiley-VCH, New York, pp 95–96
- Nugent KA, Gureyev TE, Cookson DF, Paganin D, Barnea Z (1996) Quantitative phase imaging using hard X-rays. *Phys Rev Lett* 77:2961–2964
- Park CW, Kim GB, Lee SJ (2004) Micro-PIV measurements of blood flow in a microchannel. In: International symposium on biomedical optics, San Jose, USA, Jan 24–29: #5325-09

- Pogany A, Gao D, Wilkins SW (1997) Contrast and resolution in imaging with a microfocus X-ray source. *Rev Sci Instrum* 68:2774–2782
- Snigirev A, Snigireva I, Kohn V, Kuznetsov S, Schelokov I (1995) On the possibilities of X-ray phase contrast microimaging by coherent high-energy synchrotron radiation. *Rev Sci Instrum* 66:5486–5492
- Spanne P, Raven C, Snigireva I, Snigirev A (1999) In-line holography and phase-contrast microtomography with high energy X-rays. *Phys Med Biol* 44:741–749
- Syoten O (1981) *Cardiovascular Hemorheology*. Cambridge University Press, Cambridge, pp 40–43